Killian, J. A., Burger, K. N. J., & De Kruijff, B. (1987) *Biochim. Biophys. Acta 897*, 269–284.

Killian, J. A., Prasad, K. U., Hains, D., & Urry, D. W. (1988) *Biochemistry 27*, 4848–4855.

Masotti, L., Spisni, A., & Urry, D. W. (1980) *Cell Biophys. 2*, 241–251.

Pasquali-Ronchetti, I., Spisni, A., Casali, E., Masotti, L., & Urry, D. W. (1983) *Biosci. Rep. 3*, 127–133.

Sarges, R., & Witkop, B. (1965a) *J. Am. Chem. Soc. 87*, 2011–2027.

Sarges, R., & Witkop, B. (1965b) *J. Am. Chem. Soc. 87*, 2027–2030.

Sarges, R., & Witkop, B. (1965c) *Biochemistry 4*, 2491–2494.

Seelig, J. (1978) *Biochim. Biophys. Acta 515*, 104–123.

Spisni, A., Pasquali-Ronchetti, I., Casali, E., Lindner, L., Cavatorta, P., Masotti, L., & Urry, D. W. (1983) *Biochim. Biophys. Acta 732*, 58–68.

Stark, G., Strassle, M., & Tackaz, Z. (1986) *J. Membr. Biol. 89*, 23–27.

Tilcock, C. P. S. (1986) *Chem. Phys. Lipids 40*, 109–125.

Tournois, H., Killian, J. A., Urry, D. W., Bokking, O. R., De Gier, J., & De Kruijff, B. (1987) *Biochim. Biophys. Acta 905*, 222–226.

Urry, D. W. (1985a) in *The Enzymes of Biological Membranes* (Martonosi, A. N., Ed.) 2nd ed., Vol. 1, pp 229–257, Plenum, New York.

Urry, D. W. (1985b) in *Modern Physical Methods in Biochemistry, Part A* (Neuberger/Van Deenen, Eds.) pp 266–346, Elsevier Science Publishers, B.V., New York.

Urry, D. W. (1988) *Bull. Magn. Reson. 9*, 109–131.

Urry, D. W., Long, M. M., Jacobs, M., & Harris, R. D. (1975) *Ann. N.Y. Acad. Sci. 264*, 203–220.

Urry, D. W., Spisni, A., & Khaled, M. A. (1979) *Biochem. Biophys. Res. Commun. 88*, 940–949.

Urry, D. W., Trapane, T. L., & Prasad, K. U. (1983) *Science (Washington, D.C.) 221*, 1064–1067.

Van Echteld, C. J. A., De Kruijff, B., Verkleij, A. J., Leunissen-Bijvelt, J., & De Gier, J. (1982) *Biochim. Biophys. Acta 692*, 126–138.

Veatch, W. R., & Blout, E. R. (1974) *Biochemistry 13*, 5257–5263.

Wallace, B. A. (1986) *Biophys. J. 49*, 295–306.

Weinstein, S., Wallace, B. A., Blout, E. R., Morrow, J. S., & Veatch, W. (1979) *Proc. Natl. Acad. Sci. U.S.A. 76*, 7230–7234.

Inhibition of Arginine Aminopeptidase by Bestatin and Arphamenine Analogues. Evidence for a New Mode of Binding to Aminopeptidases[†]

Scott L. Harbeson[‡] and Daniel H. Rich*

School of Pharmacy, University of Wisconsin—Madison, 425 North Charter Street, Madison, Wisconsin 53706

Received February 25, 1988; Revised Manuscript Received May 31, 1988

ABSTRACT: The synthesis and inhibition kinetics of a new, potent inhibitor of arginine aminopeptidase (aminopeptidase B; EC 3.4.11.6) are reported. The inhibitor is a reduced isostere of bestatin in which the amide carbonyl is replaced by the methylene ($-CH_2-$) moiety. Analysis of the inhibition of arginine aminopeptidase by this inhibitor according to the method of Lineweaver and Burk yields an unusual noncompetitive double-reciprocal plot. The replot of the slopes versus [inhibitor] is linear ($K_{is} = 66$ nM), but the replot of the y intercepts ($1/V$) versus [inhibitor] is hyperbolic ($K_{ii} = 10$ nM, $K_{id} = 17$ nM). These results provide evidence for a kinetic mechanism in which the inhibitor binds to the S_1' and S_2' subsites on the enzyme, not the S_1 and S_1' subsites occupied by dipeptide substrates. Furthermore, structure–activity data for a series of ketomethylene dipeptide isosteres in which the amide ($-CONH-$) of a dipeptide is replaced with the ketomethylene ($-COCH_2-$) moiety show that the S_1 and S_1' subsites preferentially bind basic and aromatic side chains, respectively. These results are in agreement with the known substrate specificity of arginine aminopeptidase. The structure–activity data for several bestatin analogues, however, show that these compounds do not bind to the S_1 and S_1' sites of arginine aminopeptidase. A comparison of the data provides evidence that bestatin inhibits arginine aminopeptidase and possibly other aminopeptidases by binding to the S_1' and S_2' sites of the enzyme.

Aminopeptidases are hydrolytic enzymes that catalyze the removal of the amino-terminal residue from a peptide chain. The inhibition of aminopeptidases has been of interest since the isolation of bestatin **1** (Figure 1) (Umezawa et al., 1976a; Suda et al., 1976), a natural product found in culture filtrates of *Streptomyces olivoreticuli*, which potently inhibits aminopeptidase enzymes from a variety of sources. Bestatin has also been reported to have therapeutically useful effects both in vivo and in vitro (Umezawa et al., 1976b; Umezawa, 1984; Shimamura et al., 1984). Our studies of aminopeptidases have involved not only investigations into the mechanism of inhibition of these enzymes by bestatin but also synthetic studies toward the preparation of new inhibitors of aminopeptidases.

Our studies of one particular aminopeptidase, arginine aminopeptidase[1] [EC 3.4.11.6; L-Arginyl (L-Lysyl)peptide hy-

1 Bestatin $(K_i = 14$ nM$)$

2 Arphamenine A $(R = H)$ $(K_i = 2.5$ nM$)^a$
3 Arphamenine B $(R = OH)$ $(K_i = 0.84$ nM$)^a$

4 X=Val $(K_i = 10$ uM$)^b$
5 X= Ile $(K_i = 3.2$ uM$)$

6 Lysine thiol $(K_i = 0.91$ nM$)^c$

7 Reduced Bestatin Isostere
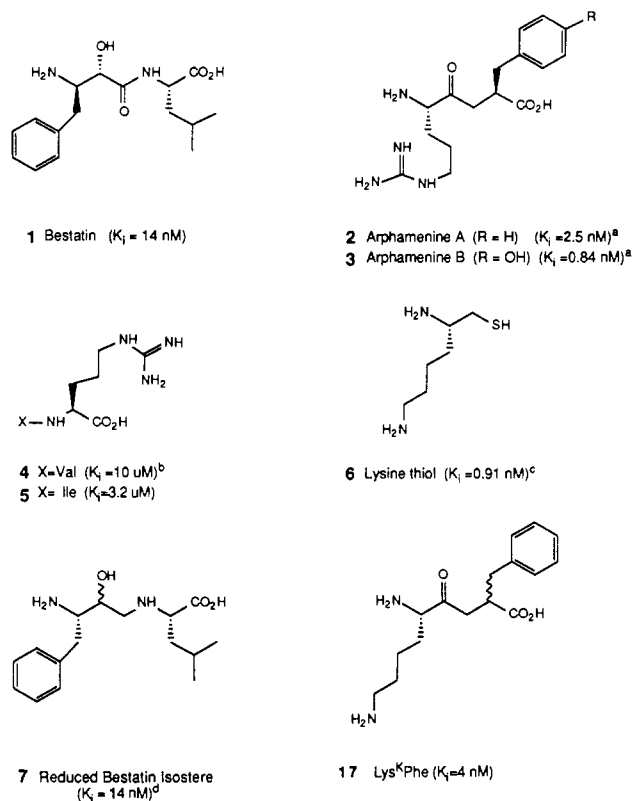$(K_i = 14$ nM$)^d$

17 Lys^{K}Phe $(K_i = 4$ nM$)$

FIGURE 1: Inhibitors of arginine aminopeptidase. Footnotes: (a) From Umezawa et al. (1984). (b) From Yamamoto et al. (1980). (c) From Ocain and Rich (1987). (d) Assayed in the absence of 0.2 M NaCl.

FIGURE 2: Mechanisms of inhibition of arginine aminopeptidase by bestatin as proposed by (a) Takita et al. (1977) and (b) Nishino and Powers (1979).

drolase], have yielded new, important mechanistic information regarding how bestatin binds to the enzyme. Arginine aminopeptidase is a cytosolic enzyme isolated from rat liver (Hopsu et al., 1966a, that appears to be composed of a single polypeptide chain of approximately 90 000-dalton molecular mass and that specifically cleaves amino-terminal arginyl or lysyl residues. Arginine aminopeptidase was originally proposed to be a zinc metalloenzyme like cytosol aminopeptidase [EC 3.4.11.1; α-aminoacyl-peptide hydrolase (cytosol) from porcine kidney] (Spackman et al., 1954) and microsomal aminopeptidase [EC 3.4.11.2; α-aminoacyl-peptide hydrolase (microsomal) from porcine kidney] (Wacker et al., 1971). A similarity of catalytic mechanisms also seems likely since all three enzymes are potently inhibited by bestatin. However, when atomic absorption was used to measure the zinc content of rat liver arginine aminopeptidase (Söderling & Mäkinen, 1983), no zinc was detected. Söderling and Mäkinen concluded that arginine aminopeptidase cannot be classified as a metallopeptidase and that sulfhydryl and imidazole groups are the essential catalytic groups of this enzyme. This interpretation conflicted with the proposed mechanism for bestatin inhibition of aminopeptidases which requires interaction of the inhibitor with a divalent cation bound at the active site (Takita et al., 1977). Recently, Ocain and Rich (1987) reported that arginine aminopeptidase is inhibited by L-lysine thiol **6**, a compound that would be expected to inhibit the

enzyme by interaction with a catalytic zinc ion in the active site.

In order to gain greater understanding of the mechanism of inhibition of arginine aminopeptidase by the aminopeptidase inhibitors in Figure 1 and perhaps even the catalytic mechanism of the enzyme, we have synthesized several analogues of bestatin **1** and arphamenines **2** and **3** and assayed them as inhibitors of the enzyme. Compound **7** is an analogue of bestatin in which the amide bond of bestatin is replaced with the aminomethylene group (-CH$_2$NH), an amide bond replacement first introduced by Szelke for use in inhibitors of renin (Szelke et al., 1982). Compound **7** was prepared to distinguish between two proposals for the mechanism of inhibition of aminopeptidases by bestatin (Figure 2). Takita et al. proposed that the α-hydroxyl and β-amino groups of bestatin chelate the zinc atom in the active site of aminopeptidases, whereas Nishino and Powers (1979) proposed that chelation involves the amide carbonyl and the α-hydroxy group. In addition, we prepared a series of inhibitors from peptides that incorporated hydrolytically stable amide bond replacements (Harbeson, 1986). These compounds contain the ketomethylene moiety (-COCH$_2$-) and are analogues of the naturally occurring arginine aminopeptidase inhibitors, arphamenines A and B (**2** and **3**, respectively). The inhibition kinetics of **7** in addition to the structure–activity data for a series of ketomethylene inhibitors and bestatin analogues reveal a new, heretofore unsuspected binding interaction between arginine aminopeptidase and bestatin. The data presented here will support the proposal that, in contrast to a substrate that binds to the S$_1$ and S$_1'$ sites of arginine aminopeptidase [the definitions for S$_1$, S$_1'$, P$_1$, P$_1'$, etc., follow the conventions of Schechter and Berger (1967)], compound **7** and bestatin **1** inhibit arginine aminopeptidase by binding to the S$_1'$ and S$_2'$ sites of the enzyme (Figure 3).

MATERIALS AND METHODS

Materials. Cytosol aminopeptidase was obtained from Sigma as a chromatographically purified suspension in 2.9 M ammonium sulfate, 0.1 M Tris, pH 8, and 5 mM magnesium chloride. Microsomal aminopeptidase was also obtained from Sigma as a suspension in 3.5 M ammonium sulfate, pH 7.7, and 10 mM magnesium chloride. L-Leucine p-nitroanilide hydrochloride, L-arginine p-nitroanilide dihydrochloride, Trizma base, MOPS,[1] epoxy-activated Sepharose 4B, EDC, and DTT were also obtained from Sigma. ω-Aminohexyl-Sepharose 6B was obtained from Pharmacia.

Enzyme Assays. All initial velocities were measured as the release of p-nitroaniline at 405 nm $(E = 9620$ mol^{-1} cm^{-1}; Tuppy et al., 1962). Assays were performed on a Gilford Model 250 spectrophotometer with a Gilford Model 6051 recorder. Both cytosol aminopeptidase and microsomal aminopeptidase were assayed by using L-leucine p-nitroanilide hydrochloride as the substrate. Cytosol aminopeptidase was diluted 10-fold into 0.10 M Tris, pH 8.5, and 5 mM magne-

[1] Abbreviations: DEAE, diethylaminoethyl; DTT, dithiothreitol; EDC, 1-ethyl-3-[(dimethylamino)propyl]carbodiimide; NMR, nuclear magnetic resonance; MOPS, 3-(N-morpholino)propanesulfonic acid; PIPES, piperazine-N,N'-bis(2-ethanesulfonic acid); Tris, tris(hydroxymethyl)aminomethane. Enzyme nomenclature follows the recommendations of the International Union of Biochemistry Nomenclature Committee (1984); therefore, aminopeptidase B, leucine aminopeptidase, and aminopeptidase M are designated as arginine aminopeptidase, cytosol aminopeptidase, and microsomal aminopeptidase, respectively.
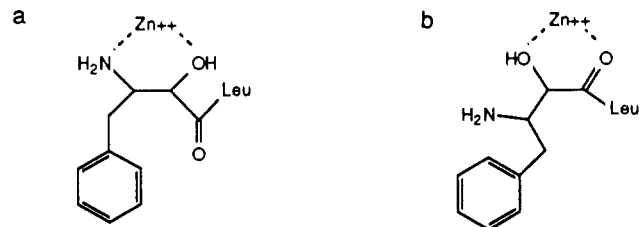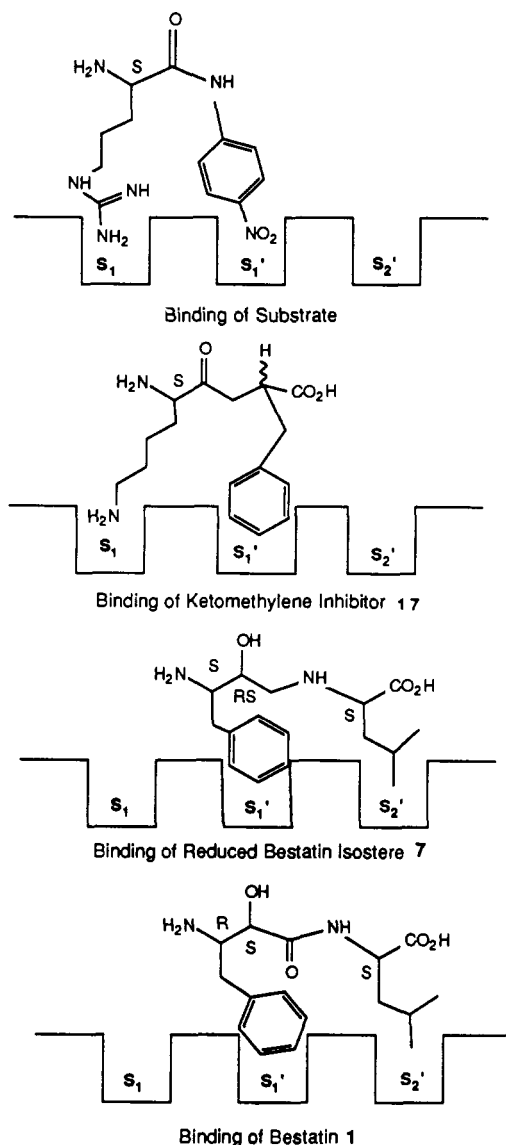
FIGURE 4: Affinity supports used in purification of arginine amino-peptidase (see supplementary material for synthesis of ligands).

FIGURE 3: Proposed binding modes to catalytic site of arginine aminopeptidase.

Data Analyses. Kinetic analyses of the data were performed on a Northstar Horizon utilizing RAGASSEK, a regression and graphical analysis package prepared by Dr. Dexter B. Northrop that utilizes a nonlinear regression routine written by Dr. Ronald G. Duggleby (Duggleby, 1984). Initial velocities are reported as μmol/(min·mg) (specific activity, units/mg). In all cases, the data were first fit line by line to the hyperbolic form of the Michaelis–Menten equation (Michaelis & Menten, 1913) (eq 1) to generate a double-reciprocal plot (Lineweaver & Burk, 1934). The slope and intercept values were then used in a regression to determine the presence or absence of slope-linear (eq 2), intercept-linear (eq 3), and intercept-hyperbolic effects (eq 7). The data were then refit to the appropriate kinetic pattern: competitive (eq 4), noncompetitive (eq 5), and slope-linear/intercept-hyperbolic noncompetitive (eq 6). These are the kinetic values that are reported.

$$v = VS/(K_m + S) \tag{1}$$

$$V/K = V/K_m(1 + I/K_{is}) \tag{2}$$

$$V = V/(1 + I/K_{ii}) \tag{3}$$

$$v = VS/[K_m(1 + I/K_{is}) + S] \tag{4}$$

$$v = VS/[K_m(1 + I/K_{is}) + S(1 + I/K_{ii})] \tag{5}$$

$$v = VS/[K_m(1 + I/K_{is}) + S(1 + I/K_{ii})/(1 + I/K_{id})] \tag{6}$$

$$V = V/[(1 + I/K_{ii})/(1 + I/K_{id})] \tag{7}$$

Syntheses. The procedure for synthesizing the reduced bestatin isostere **7** and the ligands used in the preparation of the affinity chromatography supports shown in Figure 4 can be found in the supplementary material (see paragraph at end of paper regarding supplementary material). The coupling of the affinity ligands to the supports was carried out as follows.

[(*2S,3R*)-*3-Amino-2-hydroxy-5-methylhexanoyl*]-L-*phenylalanylcysteamine–Epoxy-Activated Sepharose 6B* (**35**). This affinity chromatography support was prepared by a procedure analogous to the methodology used by Simons and VanderJagt (1977) for coupling glutathione to epoxy-activated Sepharose 6B. Epoxy-activated Sepharose 6B (5 g) was allowed to swell in water (100 mL) for 1 h at 25 °C. The gel was isolated by suction filtration, washed with more water (300 mL) and with 0.05 M sodium phosphate buffer, pH 7 (50 mL), and then suspended in the same buffer (20 mL). The suspension was then purged with nitrogen for 15 min before adding a solution of the ligand **33** (0.256 g, 0.63 mmol) in water (2 mL). The coupling was allowed to proceed for 24 h at 37 °C on a shaker. The gel was washed with water (100

sium chloride and assayed in this buffer. Microsomal aminopeptidase was diluted 100-fold into 0.10 M MOPS, pH 7.2, and 5 mM magnesium chloride, and this buffer was used in the assays. In the enzymatic assays, the protein concentrations of cytosol aminopeptidase and microsomal aminopeptidase were 40 and 3 nM, respectively, as determined from the reported protein concentrations of the stock enzyme suspensions. Arginine aminopeptidase activity was monitored spectrophotometrically by following *p*-nitroaniline release from L-arginine *p*-nitroanilide in 0.10 M PIPES, pH 7.0, containing 0.20 M NaCl and 1 mM DTT. For the arginine aminopeptidase assays, [protein] = 4 μg/mL, as determined by the A_{280}/A_{260} ratio (Warburg & Christian, 1942) of the stock enzyme solution. The A_{280}/A_{260} ratio gave results similar to those obtained by the method of Bradford (1976) with the Bio-Rad protein assay. Assays were performed in semimicro, self-masking cuvettes (1.0-cm path length) at 25 °C. For slow-binding inhibitors, 25 μL of enzyme solution was preincubated with 100 μL of inhibitor solution for 15 min prior to initiation of the enzymatic reaction with 300 μL of substrate solution. Longer preincubation times had no effect upon the final steady-state velocities. Inhibitors that did not demonstrate slow-binding kinetics were assayed without preincubation, and hydrolysis was initiated by addition of the enzyme solution.
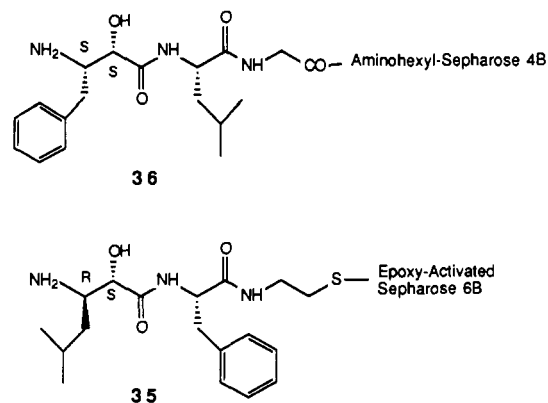
mL), resuspended in 1 M aqueous ethanolamine for 4 h at 25 °C, isolated by suction filtration, and washed with 0.5 M NaCl in 0.1 M NaOAc, pH 4 (100 mL), and finally with water (200 mL). The gel was then stored at 5 °C in 0.1% aqueous NaN₃.

[[(2S,3S)-3-Amino-2-hydroxy-4-phenylbutanoyl]-L-leucylglycyl]aminohexyl-Sepharose 4B (36). Röhm (1982) used this procedure to couple a similar ligand to ω-amino-hexyl-Sepharose for affinity chromatography of yeast aminopeptidases. The gel (5 g) was prepared allowing it to swell in 0.5 M NaCl (50 mL) for 1 h at 25 °C. The gel was isolated by suction filtration and washed well with water (200 mL). The swollen gel (17 mL) was then suspended in 50% aqueous dioxane (50 mL), and the tripeptide ligand 29 (0.20 g, 0.49 mmol) was added. The pH was adjusted to 4.8 with 0.1 N NaOH before adding EDC (1.0 g, 5.2 mmol) in several portions over a 20-min period. This mixture was stirred at 25 °C with a caged stir bar while the pH was maintained at approximately 4.8. After 7 h, the pH remained stable, and the mixture was allowed to stir 12 h. The gel was isolated by suction filtration, washed well with water (200 mL), and then stored at 5 °C in 0.1% NaN₃ (30 mL).

Purification of Arginine Aminopeptidase. The enzyme was purified by a modification of a published procedure (Hopsu et al., 1966a,b). Steps A–C are from this procedure. In step D, DEAE-Sephacel was substituted for DEAE-cellulose. The affinity chromatography steps replaced gel filtration from the original procedure. Substrates, buffers, and chromatographic media were obtained from Sigma. Chromatography was performed by using an LKB 2132 Microperpex pump and LKB 2112 Redirak fraction collector. Column elution was mounted at 278 nm with an LKB 2138 Uvicord S monitor with an LKB 2210 two-channel recorder. Protein concentrations were determined from the A_{280}/A_{260} ratio (Warburg & Christian, 1942). Activity is reported as units/mg, where 1 unit equals 1 μmol of L-arginine p-nitroanilide (0.98 mM) hydrolyzed per minute at 25 °C in 0.10 M PIPES, pH 7.0, containing 0.20 M NaCl and 1 mM DTT. Centrifugation was performed by using a Sorval RC-5B refrigerated Superspeed centrifuge equipped with an SS-34 angle rotor. Protein concentration was accomplished with either an Amicon Model 52 or Model 12 ultrafiltration cell using a YM 10 ultrafiltration membrane. All work in this purification was performed at 5 °C.

(A) Solubilization of Arginine Aminopeptidase from Rat Liver Tissue. The liver tissue (25 g) obtained from male Sprague-Dawley rats was cut into small pieces and homogenized in four portions in 50 mL of 0.10 M sodium phosphate, pH 7.0, containing 0.25 M sucrose and 1 mM DTT, by using 10 strokes of an Elvehjem–Potter homogenizer. The crude homogenates were pooled and then centrifuged for 45 min at 16000 rpm. The supernatants were then pooled to yield the crude cell-free extract (70 mL, 4480 mg, 0.0072 units/mg).

(B) Acid Precipitation at pH 5.2. The crude cell-free extract was brought to pH 5.2 by addition of cold 0.2 M HCl. After standing 15 min, the mixture was centrifuged 20 min at 20000 rpm. The supernatants were pooled and then brought to pH 7.0 by addition of cold 0.2 N NaOH (73 mL, 1600 mg, 0.013 units/mg).

(C) Ammonium Sulfate Fractionation of Arginine Aminopeptidase. Solid ammonium sulfate (17.7 g) was added to the protein solution over 30 min to give a saturated solution. This mixture was stirred 1 h before centrifugation for 20 min at 20000 rpm. The supernatants were combined and brought to 52% saturation by adding 6.06 g ammonium sulfate. This mixture was also stirred 1 h before centrifugation for 20 min

at 20000 rpm. The supernatants were discarded, and the pellets were dissolved in 10 mM sodium phosphate, pH 7.0, containing 5 mM NaCl and 1 mM DTT (15-mL total volume).

(D) DEAE-Sephacel Chromatography of Arginine Aminopeptidase. The protein solution was first desalted on a Sephadex G-25 (coarse) column (2.5 cm × 30 cm), eluting with 10 mM sodium phosphate, pH 7.0, containing 5 mM NaCl and 1 mM DTT. Those fractions containing protein were pooled (40 mL, 312 mg, 0.025 units/mg), loaded onto a DEAE-Sephacel column (2.5 cm × 60 cm), and eluted with a linear gradient of 5 mM NaCl (500 mL) to 0.50 M NaCl (500 mL) in 10 mM sodium phosphate, pH 7.0, containing 1 mM DTT. The activity peak eluted at 0.15 M NaCl. Fractions 64–73 were pooled (80 mL, 35 mg, 0.22 units/mg).

(E) Affinity Chromatography on [[(2S,3S)-3-Amino-2-hydroxy-4-phenylbutanoyl]-L-leucylglycyl]aminohexyl-Sepharose 6B (36). The pooled fractions from the preceding step were concentrated and desalted by using the Amicon Model 52 ultrafiltration cell by first reducing the volume of 10 mL, then diluting to 60 mL, and finally concentrating again to 12 mL. This solution was then loaded onto the affinity column (1 cm × 15 cm) previously equilibrated with 10 mM MOPS, pH 7.0, containing 5 mM NaCl and 1 mM DTT. The column was then washed with the same buffer (30 mL) prior to elution with a linear gradient of 5 mM NaCl (100 mL) to 1 M NaCl (100 mL) in 10 mM MOPS, pH 7.0, containing 1 mM DTT. The activity peak eluted at 0.2 M NaCl. Fractions 22–24 were pooled (12 mL, 13.4 mg, 0.46 units/mg).
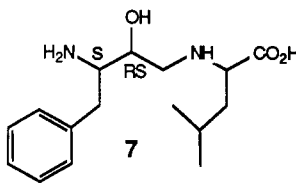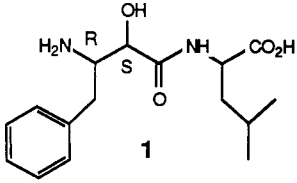
(F) Affinity Chromatography on [(2S,3R)-3-Amino-2-hydroxy-5-methylhexanoyl]-L-phenylalanylcysteamine–Epoxy-Activated Sepharose 4B (35). The enzyme solution from step E was diluted to 25 mL with 10 mM MOPS, pH 7.0, containing 1 mM DTT and then loaded onto the affinity column. The column was first washed with the same buffer (30 mL) and then eluted with a linear gradient of 5 mM NaCl (100 mL) to 0.50 M NaCl (100 mL) in this same buffer. The activity peak eluted at 0.33 M NaCl. Fractions 40–42 were pooled to yield the final enzyme preparation (12 mL, 0.60 mg, 5.0 units/mg) which had a specific activity of 5 units/mg, showed activation by NaCl, and displayed the expected substrate specificity in that it hydrolyzed L-arginine and L-lysine p-nitroanilide but not L-leucine p-nitroanilide. This preparation was used for kinetic studies.

RESULTS

Compound 7 was prepared in order to determine the importance of the amide carbonyl of bestatin for inhibition of aminopeptidases. As previously described (Figure 2), two chelation mechanisms for inhibition have been proposed: (a) coordination of the catalytic zinc by the amino and hydroxyl functions and (b) coordination by the hydroxyl and amide carbonyl. Table I shows the results obtained when the reduced bestatin isostere 7 was assayed as an inhibitor of the three enzymes. With respect to bestatin, compound 7 shows at least a 50 000-fold decrease in affinity for cytosol aminopeptidase and a 500-fold decrease for microsomal aminopeptidase. These results demonstrate a crucial role for the amide carbonyl in the mechanism of inhibition of cytosol aminopeptidase and microsomal aminopeptidase by bestatin and, at least for these two enzymes, are consistent with the additional inhibitor mechanism proposed by Nishino and Powers (Figure 2) although the amine group could be inhibiting binding.

Analysis of the inhibition of arginine aminopeptidase by the reduced bestatin isostere 7 according to the method of Lineweaver and Burk yields a double-reciprocal plot indicative

Table I: Kinetic Constants for Inhibition of Aminopeptidases by Reduced Bestatin Isostere 7, Bestatin (1), and (2S,3S)-Bestatin[a]

compounds	inhibition constants		
	cytosol APase	microsomal APase	arginine APase
7	$IC_{50} > 1$ mM	C $K_{is} = 2.1$ mM	NC(Hyper) $K_{is} = 66$ nM $K_{ii} = 10$ nM $K_{io} = 17$ nM C^{b} $K_{is} = 14$ nM
1	C $K_{is} = 20$ nM	C $K_{is} = 4.1$ μM	C $K_{is} = 14$ nM $IC_{50} = 0.16$ μM^{c}
(2S,3S)-bestatin	$K_{is} = 23$ nM		$IC_{50} = 4.1$ μM^{c}

[a] Abbreviations: APase, aminopeptidase; IC_{50}, concentration of inhibitor for 50% inhibition; C, competitive; NC(Hyper), noncompetitive, slope linear/intercept hyperbolic. [b] Assayed in the absence of added NaCl. [c] Suda et al., 1984.

of noncompetitive inhibition (Figure 5). However, this noncompetitive pattern is unusual in that the replot of the slopes versus [inhibitor] is linear whereas the replot of the y intercepts versus [inhibitor] is hyperbolic (see insets in Figure 5). When these assays were repeated in the absence of added 0.2 M NaCl in the buffer (the enzyme solution was also desalted on Sephadex G-25, coarse), the hyperbolic intercept effect is not seen and compound 7 is a potent competitive inhibitor ($K_{is} = 14$ nM) of arginine aminopeptidase (Table I). This compound represents a new class of specific, potent inhibitors of arginine aminopeptidase. The ketomethylene inhibitors (2, 3, and 16) and lysine thiol 6 are the only other potent aminopeptidase inhibitors specific for arginine aminopeptidase that have been reported.

Effects of Chloride. Arginine aminopeptidase is a chloride-activated enzyme, and when compound 7 is assayed in the absence of added 0.2 M sodium chloride, slope-linear competitive inhibition is observed ($K_{is} = 14$ nM). In the presence of added chloride, $K_{is} = 66$ nM; therefore, removal of chloride results in an apparent 4.4-fold increase in the affinity of inhibitor for free enzyme. It is noteworthy that, in the absence of added chloride, the K_{m} for substrate decreases 5-fold (from 0.15 to 0.77 mM), V_{max} decreases 2-fold (from 2.0 to 1.0 unit/mg), and V/K decreases 10-fold [from 13.1 to 1.3 units/(mg·mmol)].

DISCUSSION

Mechanism of Inhibition. Analysis of the inhibition pattern for 7 according to the tenets of Cleland (1963) suggests the inhibitor binds to two forms of the enzyme. The linear slope effect arises from the substrate and inhibitor competing for the same form of the enzyme (free enzyme). An intercept effect is observed when inhibitor and substrate bind to different forms of the enzyme which are separated by an irreversible step. The hyperbolic effect arises because inhibitor 7 does not combine in dead-end fashion but establishes an alternate, slower pathway. This reasoning is represented in Scheme I, where the mechanism of arginine aminopeptidase is shown as ordered Uni Bi. The linear slope effect is produced by formation of the dead-end EI complex. The hyperbolic intercept effect is produced by formation of an EQI complex from which Q is still released but at a slower rate than from EQ.

The rate equation for Scheme I can be derived for the simplest case by using the King–Altman method and assuming rapid-equilibrium steps for inhibitor binding (King & Altman,

Scheme I: Kinetic Mechanism for Inhibition of Arginine Aminopeptidase by the Reduced Bestatin Isostere 7
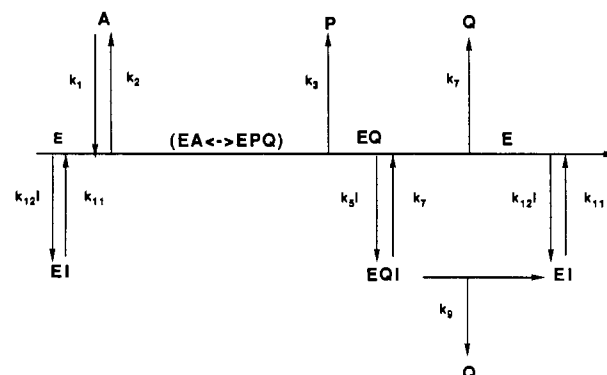
Scheme II: Derivation of the Rate Equation for the Mechanism in Scheme I[a]
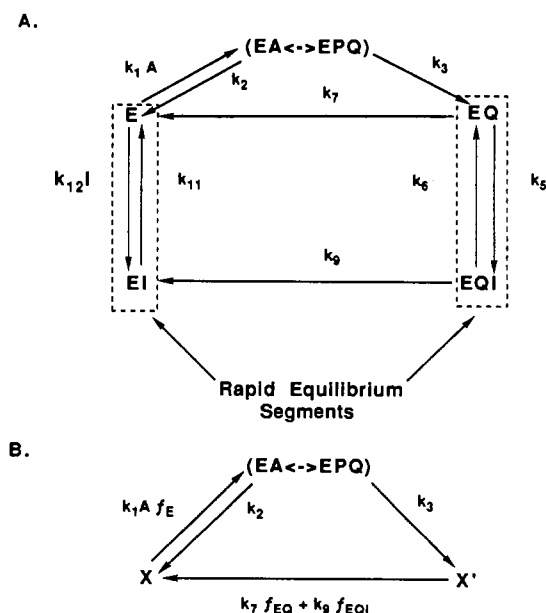
[a] (A) King–Altman pattern for Scheme I. (B) King–Altman pattern generated by assuming rapid-equilibrium binding of inhibitor 7.

1956; Cha, 1968; Huang, 1983). The application of this method is shown in Scheme II. Scheme IIA is a diagrammatic representation of the mechanism shown in Scheme I and
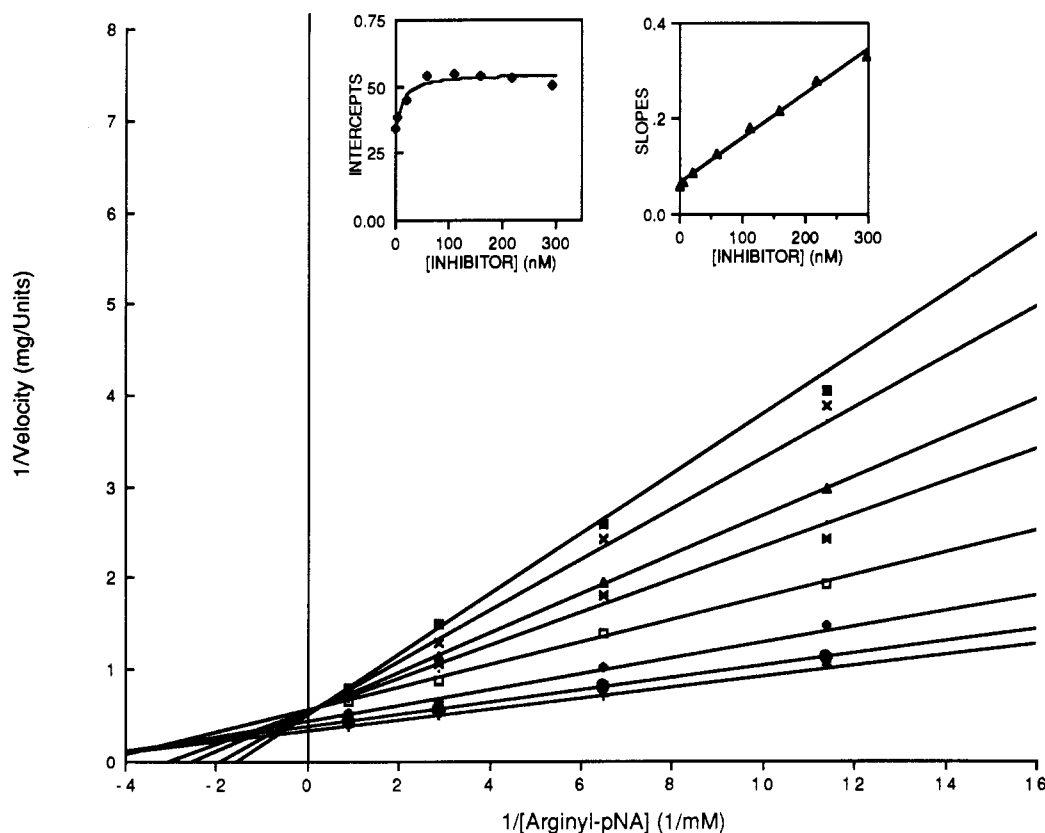
FIGURE 5: Lineweaver–Burk double-reciprocal plot of the inhibition of arginine aminopeptidase (1.2 μg, 6 × 10^{-3} units) catalyzed hydrolysis of L-arginine p-nitroanilide by compound 7. (+) 0 nM; (■) 296 nM; (×) 217 nM; (▲) 160 nM; (*) 112 nM; (□) 57.6 nM; (♦) 19.6 nM; (●) 4.93 nM. The insets display the replots of the intercept values versus [inhibitor] and of the slopes versus [inhibitor]. The data were fitted as described under Materials and Methods.

indicates the segments that are assumed to be at rapid equilibrium. The pattern that is generated is then shown in Scheme IIB in which X and X' represent the rapid-equilibrium segments, which are now treated as enzyme species. The determinants for each enzyme form are then obtained as the sum of the valid King–Altman patterns and combined to yield the rate equation:

$$v = \frac{k_3 E_0}{1 + K_a/A(1 + I/K_{is}) + k_3/k_7[(1 + I/K_{ii})/(1 + I/K_{id})]}$$

(8)

where

$$K_a = \frac{k_2 + k_3}{k_1} \qquad K_{is} = \frac{k_{11}}{k_{12}} \qquad K_{ii} = \frac{k_6}{k_5} \qquad K_{id} = \frac{k_6 k_7}{k_5 k_9}$$

Equation 8 is the most simple form for the general mechanism shown in Scheme I. The equation for inhibition of arginine aminopeptidase by 7 would be more complicated since the degree of randomness in product release is unknown and the validity of the rapid-equilibrium assumptions is unlikely since 7 is a slow-binding inhibitor. However, the rapid-equilibrium assumptions for inhibitor binding merely serve to simplify the form of the rate equation. Inclusion of slow-binding steps does not affect the kinetic mechanism. This equation does predict the linear slope and hyperbolic intercept effects and is presented as the minimal kinetic scheme that explains the results in Figure 5.

These results are interpreted in Scheme III for the inhibition of arginine aminopeptidase by reduced bestatin isostere 7. The substrate L-arginine p-nitroanilide binds to the catalytic sites S_1 and S_1'. This enzyme is an aminopeptidase so the as-

Scheme III: Diagrammatic Representation of the Kinetic Mechanism for Inhibition of Arginine Aminopeptidase by Compound 7
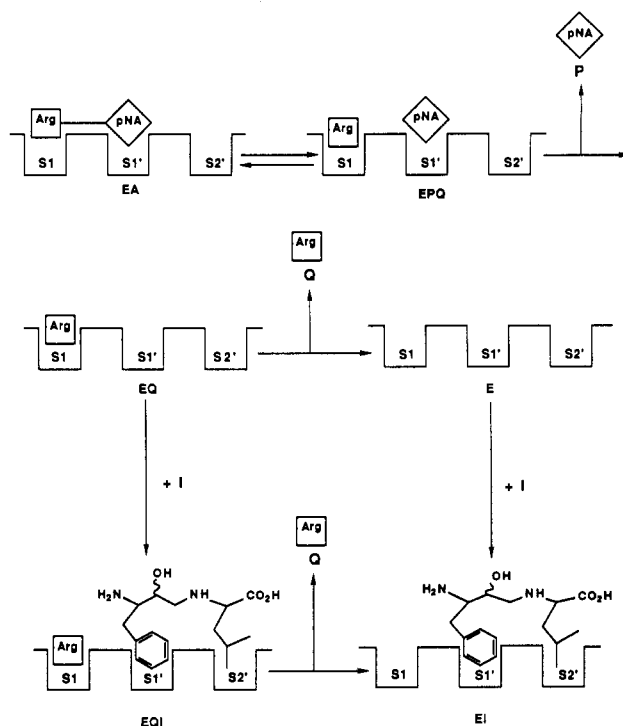
sumption is made that there is no S_2 site. After catalysis, p-nitroaniline (P) is released from S_1', which allows compound 7 to then bind at S_1' and S_2' of the EQ complex to form EQI. The slower release of L-arginine (Q) from EQI results in the

Table II

bestatin analogues

ketomethylene analogues

cmpd	*	R	R'	IC$_{50}$ (μM)	rel affinity	cmpd	R	R'	K$_i$	rel affinity
1	(S)	(R)-benzyl	i-butyl	0.16	-1.9×	14	(S)-i-butyl	CH$_3$	0.13 mM	65×
8	(S)	(R)-p-NH$_2$-benzyl	i-butyl	0.31		15	(S)-(CH$_2$)$_4$NH$_2$	CH$_3$	2.0 μM	
9	(S)	(S)-benzyl	i-butyl	4.0	negl^a	16	(S)-i-butyl	benzyl	0.17 μM	42×
10	(RS)	(S)-(CH$_2$)$_4$NH$_2$	i-butyl	4.8		17	(S)-(CH$_2$)$_4$NH$_4$	benzyl	4.0 nM	
1	(S)	(R)-benzyl	i-butyl	0.16	-25×	18	(R)-i-butyl	benzyl	0.77 μM	4.5×
9	(S)	(S)-benzyl	i-butyl	4.0		16	(S)-i-butyl	benzyl	0.17 μM	
11	(RS)	(R)-CH$_3$	i-butyl	100	620×	14	(S)-i-butyl	CH$_3$	0.13 mM	760×
1	(S)	(R)-benzyl	i-butyl	0.16		16	(S)-i-butyl	benzyl	0.17 μM	
13	(S)	(R)-benzyl	CH$_3$	1.01	-11×	15	(S)-(CH$_2$)$_4$NH$_2$	CH$_3$	2.0 μM	500×
12	(S)	(R)-benzyl	benzyl	11.2		17	(S)-(CH$_2$)$_4$NH$_2$	benzyl	4.0 nM	

^{a} Negl, negligible.

hyperbolic intercept effect. As shown by this model, the linear slope effect occurs because inhibitor and substrate both compete for E by binding to overlapping sites, not the same sites.

Proposed Mechanism for the Binding of Bestatin to Arginine Aminopeptidase. The binding of the reduced bestatin isostere 7 to S$_1$' and S$_2$' of arginine aminopeptidase suggests that bestatin also binds in an analogous fashion. This postulate is strongly supported by a comparison of structure–activity relationships for ketomethylene inhibitors with those of bestatin analogues which had been prepared and tested by Umezawa and co-workers (Takita et al., 1977). In making this comparison, the assumption is made that ketomethylene-containing dipeptide isosteres (e.g., 17, 2, 3) bind to the same sites on arginine aminopeptidase as the corresponding peptide substrates. The K_{is} values are interpreted in terms of the affinities of the enzyme subsites (i.e., S$_1$, S$_1$', S$_2$', etc.) for inhibitor side chains. These data are shown in Table II.

The ketomethylene inhibitors show three important structure–activity relationships for binding to arginine aminopeptidase. The first two entries of Table II (15 vs 14 and 17 vs 16) show that the S$_1$ subsite has a greater affinity for the lysine and the arginine side chains (arphamenines A and B have arginine side chains), a result expected for an enzyme that hydrolyzes amino-terminal lysyl and arginyl residues. The next entries (18 vs 16) show that the affinity is decreased somewhat (4.5-fold) when there is an amino-terminal D residue. This effect is not very large and agrees with the report that arginine aminopeptidase hydrolyzes D-Arg-L-Phe and D-Arg-D-Val (Hopsu et al., 1966b). The third characteristic of arginine aminopeptidase, which is shown by the last two entries (14 vs 16 and 15 vs 17), is that there is a pronounced affinity for aromatic residues at the S$_1$' site. This specificity has also been demonstrated (Söderling, 1983) for substrates, although the effect is not as large. Arg-Phe is a better substrate than Arg-Gly (k_{cat}/K_m = 371 and 110 mM^{-1} s^{-1} and k_{cat} = 1960 and 1256 s^{-1}, respectively), and Söderling has noted that the hydrophobicity of the C-terminal residue of a dipeptide substrate plays an important role in substrate catalysis and affinity. Our results with the ketomethylene dipeptides establish that an aromatic residue binding to S$_1$' can have a large effect upon the binding affinity of inhibitors.

Examination of the data in Table II reveals that the structure–activity data for bestatin and its analogues do not agree with those for the ketomethylene inhibitors if bestatin is considered to bind in an analogous fashion to the S$_1$-S$_1$' enzyme sites. The first two entries (1 vs 8 and 9 vs 10) fail

to show the increase in binding expected from introduction of an amino-terminal residue bearing a protonated amine functionality. It can be argued that the p-aminobenzyl group (compound 8) is a poor analogue of lysine, but when this residue is replaced by a lysine side chain (compound 10), there is a negligible effect on the IC$_{50}$. An increase in affinity of 25-fold is seen with the R configuration at the amino terminus (1 vs 9), which contradicts the stereochemical specificity shown for the ketomethylene substrate analogues. The last two entries contain the most compelling evidence that bestatin does not bind to the same sites as a dipeptide substrate. These data clearly show that introduction of an aromatic residue at the amino terminus (10 vs 1) produces a dramatic 620-fold increase in binding affinity whereas substitution of a phenylalanine for the second residue (12 vs 13) produces an 11-fold decrease in affinity. *We propose, therefore, that ketomethylene dipeptide isosteres bind to the S$_1$ and S$_1$' sites of arginine aminopeptidase but that the reduced bestatin isostere 7, bestatin, and its analogues bind to S$_1$' and S$_2$' and exert their potent inhibitory effects at these sites (Figure 3).*

An apparent contradiction to this binding mode for bestatin is the absence of a hyperbolic intercept effect when bestatin is assayed as an inhibitor of arginine aminopeptidase, but there are two likely explanations for its absence. Bestatin may not bind to the EQ complex; therefore, it would have no effect upon the rate of release of the second product, Q. Bestatin contains an amide bond which would make the structure more rigid than 7, and this increased rigidity could prevent bestatin from binding to S$_1$' and S$_2$' while S$_1$ is still occupied by the second product. Another possibility is that bestatin does bind to EQ but has little or no effect upon the rate of release of the second product. In this case the formation of an EQI complex would be kinetically invisible.

This same reasoning may apply to the observed effects of chloride upon the inhibition kinetics of 7. In the absence of 0.2 M NaCl, 7 behaves as a competitive inhibitor of arginine aminopeptidase. This loss of the intercept effect may be due to a change in the order of product release. If, in the absence of chloride, Q is released prior to P, then neither an EQ nor an EQI complex could form. If no EQI complex is formed, then no intercept effect would be observed. Another possibility is that, in the absence of chloide, the formation of the EQI complex is kinetically invisible. We observed that 0.2 M NaCl results in a 2-fold increase in V_{max} for arginine aminopeptidase catalyzed hydrolysis of L-Arg-pNA and that inhibition by 7 results in a 1.9-fold decrease in V_{max}. In the absence of

chloride, the rate of Q release from EQ and EQI may be similar, which would cause the formation of the EQI complex to be kinetically invisible.

We attempted to find other explanations for the discrepancies in the structure–activity data in Table II between bestatin and ketomethylene inhibitors. We considered if bestatin bound to S_1 and S_1' as opposed to S_1' and S_2' as we have proposed. For this binding mode to be consistent with the ketomethylene inhibitor binding, the bestatin analogues would have to bind to arginine aminopeptidase in a backward fashion (C←N rather than N→C) such that the carboxy-terminal residue occupies the S_1 subsite and the amino-terminal residue occupies the S_1' subsite. This binding orientation would place the aromatic residue of bestatin at S_1', the site that the substrate and ketomethylene data indicate has a high affinity for aromatic residues. This binding mode was rejected for several reasons. If bestatin is bound in this fashion, then the reduced bestatin isostere **7** would also be bound at the same sites. This binding mode for **7** is incompatible with the hyperbolic intercept effect observed with arginine aminopeptidase according to the kinetic mechanism proposed in Scheme I. A very convincing argument against this alternative binding mode for bestatin is also provided by a bestatin analogue in which the carboxy-terminal residue is replaced by a lysine residue (Takita et al., 1977). The alternate binding mode predicts that this compound should be a very good inhibitor since an aromatic residue would occupy S_1' and a lysyl residue would occupy S_1; however, this compound is inactive as an inhibitor of arginine aminopeptidase. For these reasons we have discarded the possibility that bestatin binds in a backward fashion to S_1 and S_1' of arginine aminopeptidase and conclude that bestatin must exert its inhibitory effect by binding at the S_1' and S_2' sites of the enzyme.

Bestatin Binding to Aminopeptidases in General. The way that bestatin binds to arginine aminopeptidase may extend to the mechanism of inhibition of aminopeptidases by bestatin in general. Although the catalytic mechanism of arginine aminopeptidase is still the subject of debate, our proposed binding mode for bestatin may also occur during inhibition of other aminopeptidases such as cytosol aminopeptidase and microsomal aminopeptidase. The results obtained for the reduced bestatin isostere **7** with both the cytosol and microsomal aminopeptidases show that the amide carbonyl is critical for inhibitory activity. These results may support the proposal that bestatin inhibition depends upon chelation of the catalytic zinc by the amide carbonyl and α-hydroxyl moieties (Figure 2). However, the results obtained for arginine aminopeptidase suggests an alternative binding mode for bestatin with aminopeptidases that may not require a chelation of the catalytic zinc by bestatin. In view of this alternate binding mode, the poor inhibitory activity for compound **7** with the other aminopeptidases may be due to something other than the inability to chelate the catalytic zinc. The amide carbonyl may be required for some other important interaction with the protein, such as a hydrogen bond, or the loss of inhibitory activity may be due to introduction of a basic, secondary amine in place of an amide nitrogen, with the enzymes unable to tolerate the resulting positive charge.

The general assumption in the literature has been that bestatin behaves as a transition-state analogue inhibitor of aminopeptidases with the tetrahedral carbon bearing the hydroxyl group (C-2) mimicking the tetrahedral intermediate formed during enzyme-catalyzed hydrolysis of the substrate (Takita et al., 1977; Ricci et al., 1982; Nishino & Powers, 1979). In accordance with the original mechanism for cytosol
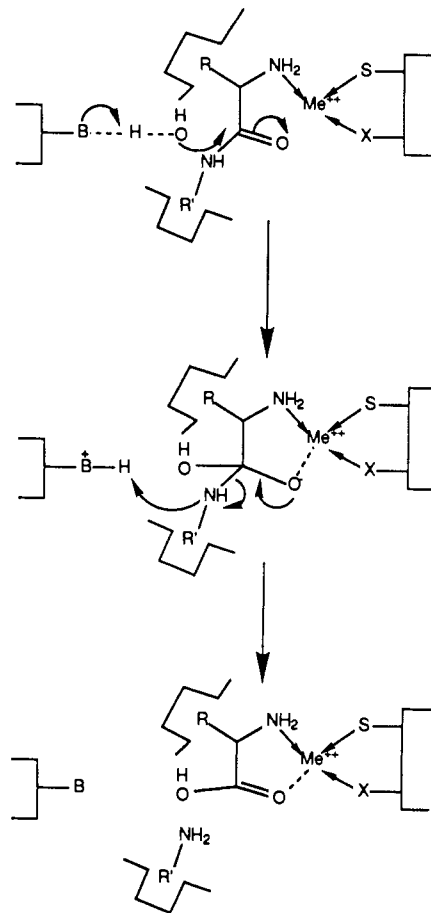

FIGURE 6: Mechanism of cytosol aminopeptidase catalyzed hydrolysis of an amide bond as proposed by Bryce and Rabin (1964a,b).

aminopeptidase as shown in Figure 6 (Bryce & Rabin, 1964a,b), an interaction of the bestatin hydroxyl with the zinc cation bound to the catalytic site has been invoked in the transition-state analogue models (see Figure 2). Several recent studies, however, have provided evidence that the hydroxyl is not interacting with the catalytic zinc and that the tetrahedral carbon bearing the hydroxyl is not mimicking the tetrahedral center formed during enzyme-catalyzed hydrolysis. A bestatin analogue, thiobestatin **20** (Figure 7), was prepared both in our lab (Ocain & Rich, 1988) and by researchers at Squibb (Gordon et al., 1987), in which the bestatin hydroxyl group was replaced with a thiol group in order to increase the affinity of bestatin for the zinc cation and increase inhibitor potency. Results obtained with arginine aminopeptidase (Ocain & Rich, 1987) for L-lysinol and L-lysine thiol **6** ($K_i = 1$ mM and 0.91 nM, respectively) and results reported for the inhibition of microsomal aminopeptidase by L-leucinol ($K_i = >5$ mM; Chan et al., 1982) and L-leucine thiol **19** ($K_i = 51$ nM; Chan et al., 1985) indicated that the substitution of a thiol for the hydroxyl of bestatin should result in a significant increase in inhibitor potency, but in fact this substitution gave only a modest (3–13-fold for **20**) increase in binding affinity. In another example, Giannousis and Bartlett (1987) have described the synthesis of a bestatin analogue in which the tetrahedral carbon bearing the hydroxyl is replaced with a tetrahedral phosphorus center (compound **21**, Figure 7); this compound was only moderately active as an inhibitor of cytosol aminopeptidase.

The poor inhibition observed with compounds **20** and **21** is consistent with the proposed binding of bestatin to the S_1' and S_2' sites of the aminopeptidases. In order for bestatin to mimic the transition state for substrate hydrolysis, it must bind to the catalytic site in a fashion analogous to the binding of a
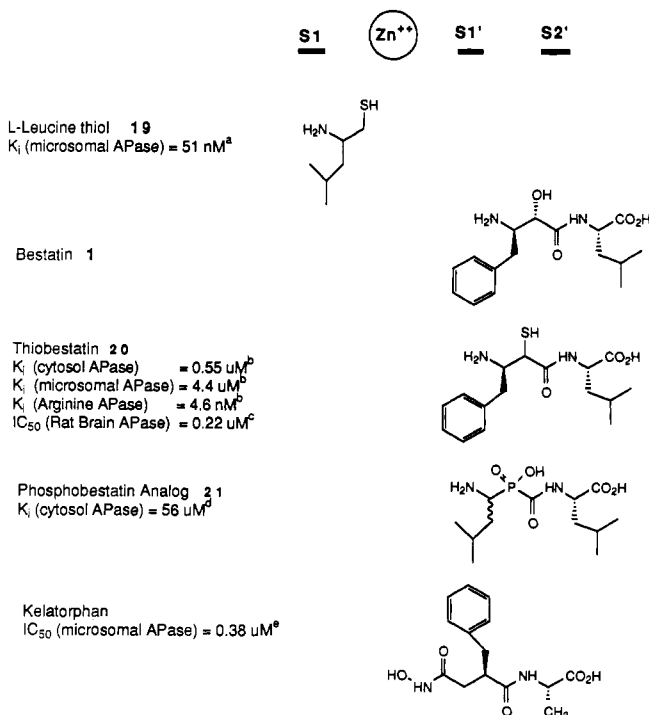
S1 (Zn⁺⁺) S1' S2'

L-Leucine thiol **19**
K_i (microsomal APase) = 51 nM[a]

Bestatin **1**

Thiobestatin **20**
K_i (cytosol APase)   = 0.55 uM[b]
K_i (microsomal APase) = 4.4 uM[b]
K_i (Arginine APase)   = 4.6 nM[b]
IC_{50} (Rat Brain APase) = 0.22 uM[c]

Phosphobestatin Analog **21**
K_i (cytosol APase) = 56 uM[d]

Kelatorphan
IC_{50} (microsomal APase) = 0.38 uM[e]

FIGURE 7: Possible modes of binding of L-leucine thiol, bestatin, thiobestatin, phosphobestatin, and kelatorphan to cytosol aminopeptidase. Footnotes: (a) Data from Chan et al. (1985). (b) Data from Ocain and Rich (1988). (c) Data from Gordon et al. (1987). (d) Data from Giannousis and Bartlett (1987). (e) Data from Fournie-Zaluski et al. (1984).

substrate, so that the C-2 hydroxyl group is between S_1 and S_1' in the same orientation as the tetrahedral intermediate formed during amide bond hydrolysis. If, as our data have shown for arginine aminopeptidase, bestatin binds at the S_1' and S_2' sites of other aminopeptidases, then the analogy to the tetrahedral intermediate is lost. Therefore, compound **21** would not be expected to be a potent inhibitor of cytosol aminopeptidase.

Binding of bestatin to the S_1' and S_2' sites moves the tetrahedral center bearing the hydroxyl into another region of the active site and alters the nature of the interaction of the hydroxyl with the catalytic zinc. Whether such an interaction actually occurs or not is unknown. If it does, it is likely to do so by a mechanism more in line with that proposed for inhibition of aminopeptidases by kelatorphan (Fournie-Zaluski et al., 1984) in which the potential zinc ligand approaches the active site zinc ion from the S_1' side rather than approaching the metal ion from the S_1 side as do leucine thiol **19** and lysine thiol **6** (see Figure 7). Substitution of a thiol for the hydroxyl of bestatin, therefore, would not necessarily be expected to increase inhibitor potency to the extent observed for **6** and **19** since the geometries of their respective interactions with the catalytic zinc would be so different. The role of the 2S hydroxyl group in bestatin remains to be established. The group is essential, as is evident from the loss of activity when it is deleted (Rich et al., 1984). Replacing the hydroxyl by thiol provides modest increases in binding, suggesting that some interaction between the zinc ion and thiol is occurring; however, the increased potency is far less than observed for either **19** or **6**, so that any interaction must be significantly weakened. One possibility is that the 2S hydroxyl group of bestatin replaces a water molecule in the active site of the enzyme (possibly substrate water) which either does not interact with the catalytic zinc ion or else interacts only at the expense of other interactions that stabilize the enzyme-inhibitor complex.

The results presented here should serve as a basis for reevaluation of the mechanism of binding of bestatin to other aminopeptidases and should be an important consideration in proposed models for inhibition of aminopeptidases by bestatin.

SUPPLEMENTARY MATERIAL AVAILABLE

Procedures for synthesizing the reduced bestatin isostere **7** and the ligands used in the preparation of the affinity chromatography supports shown in Figure 4 (13 pages). Ordering information is given on any current masthead page.

REFERENCES

Bradford, M. (1976) *Anal. Biochem. 72*, 248–254.
Bryce, G. F., & Rabin, B. R. (1964a) *Biochem. J. 90*, 509–512.
Bryce, G. F., & Rabin, B. R. (1964b) *Biochem. J. 90*, 513–519.
Cha, S. (1968) *J. Biol. Chem. 243*, 820.
Cleland, W. W. (1963) *Biochim. Biophys. Acta 67*, 173.
Duggleby, R. G. (1984) *Comput. Biol. Med. 14*, 447–455.
Fournie-Zaluski, M. C., Chaillet, P., Bouboutou, R., Coulaud, A., Cherot, P., Waksman, G., Costentin, J., & Roques, B. P. (1984) *Eur. J. Pharmacol. 102*, 525–528.
Giannousis, P. P., & Bartlett, P. A. (1987) *J. Med. Chem. 30*, 1603–1609.
Gordon, E. M., Godfrey, J. D., Delaney, N. G., Asaad, M., & Von Langen, D. (1987) Abstracts of the 10th American Peptide Symposium, St. Louis, May 23–28, 1987, Poster P-119.
Harbeson, S. L. (1986) Ph.D. Thesis, University of Wisconsin, Madison, WI.
Hopsu, V. K., Mäkinen, K. K., & Glenner, G. G. (1966a) *Arch. Biochem. Biophys. 114*, 557–566.
Hopsu, V. K., Mäkinen, K. K., & Glenner, G. G. (1966b) *Arch. Biochem. Biophys. 114*, 567–575.
Huang, C. Y. (1983) in *Contemporary Enzyme Kinetics and Mechanism* (Purich, D. L., Ed.) pp 1–32, Academic, Orlando, FL.
King, E. L., & Altman, C. (1956) *J. Phys. Chem. 60*, 1375.
Lineweaver, H., & Burk, D. (1934) *J. Am. Chem. Soc. 56*, 658.
Michaelis, L., & Menten, M. L. (1913) *Biochem. Z. 49*, 333.
Nishino, N., & Powers, J. C. (1979) *Biochemistry 18*, 4340–4347.
Ocain, T., & Rich, D. H. (1987) *Biochem. Biophys. Res. Commun. 145*, 1038–1042.
Ocain, T., & Rich, D. H. (1988) *J. Med. Chem.* (in press).
Ricci, J. S., Jr., Bousvaros, A., & Taylor, A. (1982) *J. Org. Chem. 47*, 3063–3065.
Rich, D. H., Moon, B. J., & Harbeson, S. (1984) *J. Med. Chem. 27*, 417–422.
Röhm, K.-H. (1982) *Hoppe-Seyler's Z. Physiol. Chem. 363*, 641–649.
Schechter, I., & Berger, A. (1967) *Biochem. Biophys. Res. Commun.* 157–162.
Shimamura, M., Hazato, T., & Katayama, T. (1984) *Biochim. Biophys. Acta 798*, 8.
Simons, P. C., & VanderJagt, D. L. (1977) *Anal. Biochem. 82*, 334–341.
Söderling, E. (1983) *Arch. Biochem. Biophys. 220*, 1–10.

Söderling, E., & Mäkinen, K. K. (1983) *Arch. Biochem. Biophys. 220*, 11–21.

Spackman, D. H., Smith, E. L., & Brown, D. M. (1954) *J. Biol. Chem. 212*, 255–299.

Suda, H., Takita, T., Aoyagi, T., & Umezawa, H. (1976) *J. Antibiot. 29*, 100–102.

Szelke, M., Jones, D. J., & Hallett, A. (1982) *European Patent Appl.* EP 45665.

Takita, T., Nishizawa, R., Saino, T., Suda, H., Aoyagi, T., & Umezawa, H. (1977) *J. Med. Chem. 20*, 510–515.

Tuppy, H., Wiesbauer, W., & Wintersberger, E. (1962) *Hoppe-Seyler's Z. Physiol. Chem. 329*, 278–288.

Umezawa, H. (1984) *Drugs Exp. Clin. Res. 10*, 519–531.

Umezawa, H., Aoyagi, T., Suda, H., Hamada, M., & Takeuchi, T. (1976a) *J. Antibiot. 29*, 97–99.

Umezawa, H., Ishizuka, M., Aoyagi, T., & Takeuchi, T. (1976b) *J. Antibiot. 29*, 857–859.

Umezawa, H., Aoyagi, T., Ohuchi, S., Okuyama, A., Suda, H., Takita, T., Hamada, M., & Takeuchi, T. (1984) *J. Antibiot. 36*, 1572–1575.

Wacker, H., Lehky, P., Vanderhaeghe, F., & Stein, E. A. (1971) *Biochim. Biophys. Acta 54*, 473–485.

Warburg, O., & Christian, W. (1942) *Biochem. Z. 310*, 384–421.

Yamamoto, K., Suda, H., Ishizuka, M., Takeuchi, T., Aoyagi, T., & Umezawa, H. (1980) *J. Antibiot. 33*, 1597–1599.

pH Dependence of Folding of Iso-2-cytochrome *c*[†]

Barry T. Nall,* John J. Osterhout, Jr.,‡ and Latha Ramdas§

Department of Biochemistry, University of Texas Health Science Center, San Antonio, Texas 78284, and Department of Biochemistry and Molecular Biology, University of Texas Medical School, Houston, Texas 77225

ABSTRACT: Starting from a standard unfolded state (3.0 M guanidine hydrochloride, pH 7.2), the kinetics of refolding of iso-2-cytochrome *c* have been investigated as a function of final pH between pH 3 and pH 10. Absorbance in the ultraviolet and visible spectral regions and tryptophan fluorescence are used to monitor folding. Over most of the pH range, fast and slow folding phases are detected by both fluorescence and absorbance probes. Near neutral pH, the rate of fast folding appears to be the same when monitored by absorbance and fluorescence probes. At higher and lower pH, there are two fast folding reactions, with absorbance-detected fast folding occurring in a slightly faster time range than fluorescence-detected fast folding. The rates of both fast folding reactions pass through broad minima near neutral pH, indicating involvement of ionizable groups in rate-limiting steps. The rates of slow folding also depend on the final pH. At acid pH, there appears to be a single slow folding phase for both fluorescence and absorbance probes. At neutral pH, the absorbance-detected and fluorescence-detected slow folding phases separate into distinct kinetic processes which differ in rate and relative amplitude. At high pH, absorbance-detected slow folding is no longer observed, while fluorescence-detected slow folding is decreased in amplitude. In contrast, the equilibrium and kinetic properties of proline imide bond isomerization, believed to be involved in the slow folding reactions, are largely independent of pH. The results suggest that the pH dependence of slow folding involves coupling of pH-sensitive structure to proline imide bond isomerization. The dependence of kinetic properties on pH suggests that one factor governing the rates of both fast and slow folding reactions involves ionizable groups which alter the stability of folding intermediates. Differences in the pH sensitivity of key intermediates may influence relative rates and thus the selection of pathways in folding, leading to appearance and disappearance of kinetic phases.

Protein folding is often viewed as a relatively simple reaction. Folding starts in an unfolded state composed of astronomical numbers of unstructured polypeptide chains with similar free energies and proceeds directly to a unique (but dynamic) folded state at the global free energy minimum. This two-state view has been surprisingly successful in understanding equilibrium folding/unfolding transitions. Nevertheless, the mo-

lecular gymnastics required to fold a protein suggest considerable mechanistic complexity. Evidence of this complexity is provided by experimental observations of a multitude of kinetic phases in folding. Kinetic experiments prove that several (kinetically distinct) species are present but the importance of these species in directing the process of folding remains controversial.

Criteria for judging the importance of kinetically detected species are provided by folding to different final conditions. If the species are important in guiding folding, then changes in the final conditions should affect the relative stability of the intermediates and thus the rates and amplitudes for folding reactions. The experimental question reduces to whether or not there are qualitative differences in the kinetic patterns for folding under different final conditions.

For horse cytochrome *c*, it is well-known that the number and amplitudes of kinetic phases depend strongly on experimental conditions such as the presence or absence of external heme ligands, the type of denaturant, and pH (Brems &